UDK 551.248.2

https://doi.org/10.30730/gtrz.2025.9.1.037-055
https://www.elibrary.ru/ouzgfu

Tectonophysical digital database of Sakhalin Island*

Pavel A. Kamenev[1@], *Anton V. Marinin*[2], *Lidia A. Sim*[2], *Leonid M. Bogomolov*[1], *Anton R. Lukmanov*[2], *Vladislav A. Degtyarev*[1]

[@]*E-mail: p.kamenev@imgg.ru*

[1] *Institute of Marine Geology and Geophysics, FEB RAS, Yuzhno-Sakhalinsk, Russia*
[2] *Schmidt Institute of Physics of the Earth of RAS, Moscow, Russia*

Abstract. The paper summarizes the results of field tectonophysical studies of Sakhalin Island conducted by different researchers at different times. Information about the main characteristics of the stress-strained state of the upper part of the Earth's crust (principal stress axes, stress state type, Lode–Nadai coefficient, bedding planes) was obtained as a result of computations using methods of cataclastic analysis of discontinuous displacements, structural-paragenetic, kinematic, conjugate pairs of faults. The input data for the calculations were the materials of field measurements of fracturing, slickensides and structural patterns. The results obtained in the present and previous works on Sakhalin field tectonophysical research are represented in summary tables that include data on local stress states for 264 observation points. The results are incorporated to GIS, the Isoline GIS software is used for the database management system.

Keywords: fracturing, slickensides, stress-strained state of the Earth's crust, principal stress axes, Lode–Nadai coefficient

Тектонофизическая цифровая база данных территории острова Сахалин

П. А. Каменев[1@], *А. В. Маринин*[2], *Л. А. Сим*[2], *Л. М. Богомолов*[1], *А. Р. Лукманов*[2], *В. А. Дегтярев*[1]

[@]*E-mail: p.kamenev@imgg.ru*

[1] *Институт морской геологии и геофизики ДВО РАН, Южно-Сахалинск, Россия*
[2] *Институт физики Земли им. О.Ю. Шмидта РАН, Москва, Россия*

Резюме. База тектонофизических данных по о. Сахалин, создаваемая коллективом авторов из Института физики Земли им. О.Ю. Шмидта РАН и Института морской геологии и геофизики ДВО РАН, обобщает результаты полевых исследований деформации горных пород и геологических тел на территории острова за период с 1973 по 2023 г. Сведения об основных характеристиках напряженно-деформированного состояния верхней части земной коры (оси главных напряжений, тип напряженного состояния, коэффициент Лоде–Надаи, элементы залегания слоистости) получены в результате расчетов методами катакластического, структурно-парагенетического и кинематического анализа, а также сопряженных пар сколов. Исходными данными для расчетов служили полевые замеры параметров тектонической трещиноватости, зеркал скольжений и других структурных индикаторов деформаций. Результаты полевых тектонофизических исследований Сахалина, полученные разными исследователями в различное время, сведены в итоговые таблицы, которые включают данные о локальных стресс-состояниях для 264 точек наблюдения. Данные интегрированы с ГИС; в качестве системы управления базой данных используется программный комплекс Isoline GIS.

Ключевые слова: трещиноватость, зеркала скольжения, напряженно-деформированное состояние земной коры, оси главных напряжений, коэффициент Лоде–Надаи

* The translation from Russian: Каменев П.А., Маринин А.В., Сим Л.А., Богомолов Л.М., Лукманов А.Р., Дегтярев В.А. Тектонофизическая цифровая база данных территории острова Сахалин. *Геосистемы переходных зон*, 2025, т. 9, № 1. [Electronic resource]. http://journal.imgg.ru/web/full/f2025-1-3.pdf. *Translated by Valeria Maksimova*

Полный текст статьи на русском языке см. на сайте журнала «*Геосистемы переходных зон*»: http://journal.imgg.ru/web/full/f2025-1-3.pdf

For citation: Kamenev P.A., Marinin A.V., Sim L.A., Bogomolov L.M., Lukmanov A.R., Degtyarev V.A. Tectonophysical digital database of Sakhalin Island. *Geosistemy perehodnykh zon = Geosystems of Transition Zones*, 2025, vol. 9, no. 1, pp. 37–55. (In Russ. & in Engl.). https://doi.org/10.30730/gtrz.2025.9.1.037-055. [The translation from Russian: Каменев П.А., Маринин А.В., Сим Л.А., Богомолов Л.М., Лукманов А.Р., Дегтярев В.А. Тектонофизическая цифровая база данных территории острова Сахалин. [Electronic resource]. *Геосистемы переходных зон*, 2025, т. 9, № 1. URL: http://journal.imgg.ru/web/full/f2025-1-3.pdf].

Funding and Acknowledgements

The research was carried out with the framework of the state task of the Institute of Marine Geology and Geophysics of the Far Eastern Branch of RAS (FWWM-2021-0001) and the state task of the Schmidt Institute of Physics of the Earth of the Russian Academy of Sciences (FMWU-2025-0036). The authors are grateful to Yury V. Kostrov for his support in conducting field research. The authors express special gratitude to Vitaliy M. Yakovlev and Vyacheslav V. Yakovlev for the kindly provided software package Isoline GIS.

Финансирование и благодарности

Исследования проводились в рамках госзадания Института морской геологии и геофизики ДВО РАН (FWWM-2021-0001) и госзадания Института физики Земли им. О.Ю. Шмидта РАН (FMWU-2025-0036).
Авторы признательны Ю.В. Кострову за помощь в проведении полевых исследований. Особая благодарность В.М. Яковлеву и В.В. Яковлеву за предоставленный пакет программного обеспечения Isoline GIS.

Introduction

Tectonophysics is a relatively nascent science, yet it possesses a robust methodological framework, both independently and in conjunction with techniques from other disciplines [1]. Currently, tectonophysical methods are actively employed to address problems in geodynamics, tectonics, structural geology, geomechanics, exploration and exploitation of mineral deposits. In an applied context, only these methods enable the reconstruction of the stress-strained state of the Earth's crust, for example, at mineral deposits [2, 3]. In fundamental research, these methods assist, in particular, in refining the boundaries of tectonic plates [4].

On Sakhalin Island, tectonophysical methods were actively implemented in the coal industry in the late 20th century to predict hazardous dynamic and gasodynamic phenomena (rock bursts, coal and gas blowouts). Such events occurred at the Boshnyakovo and Lopatinskoe deposits in Sakhalin mines [2]. Subsequently, the method of cataclastic analysis of discontinuous displacements [5] was utilized to reconstruct the tectonic stresses of the island, incorporating data on earthquake focal mechanisms [6]. In recent years, field tectonophysical studies have been resumed in the articles of L.A. Sim and colleagues [4, 7, 8], and continued by researchers from the Schmidt Institute of Physics of the Earth of the Russian Academy of Sciences in collaboration with researchers from the Institute of Marine Geology and Geophysics of the Far Eastern Branch of the Russian Academy of Sciences (IMGG FEB RAS) [9, 10].

Field tectonophysical investigations on Sakhalin are conducted using GIS technologies. This has facilitated the creation of the Sakhalin Island Tectonophysical Database, registered with the Federal Service for Intellectual Property in 2024 [11]. This database encompasses research results from 2020–2023. The objective of the present work is to systematize tectonophysical information obtained using field tectonophysical methods on Sakhalin Island from 1973 to 2023, for its introduction into scientific circulation with open access to all interested researchers. This includes documenting features indicative of past deformation, such as fracturing patterns and the orientation of slickensides, allowing for calculation of principal stress axes and determination of the Lode–Nadai coefficient to characterize the deformation regime.

Area and materials of study

The geological structure of Sakhalin Island predominantly comprises Cretaceous-Cenozo-

ic sedimentary rocks with a minor proportion of volcanogenic formations [12, 13], with the exception of several formations in central and eastern Sakhalin. These exceptional formations consist of volcanogenic ultramafic and metamorphosed strata with a paleontologically validated age ranging from the Silurian to the Jurassic periods [14]. The relatively young age of the sedimentary rocks renders them highly susceptible to exogenic processes, manifesting as intense weathering. A significant part of the island is characterized by low-lying terrain lacking bedrock exposures.

The study area encompasses the entirety of Sakhalin Island where infrastructure facilitates access to outcrop locations. Beyond challenges related to transportation infrastructure, field investigations encounter further difficulties. During winter, snow cover precludes field work. In the summer season, luxuriant vegetation complicates both the detection of outcrops and access to them. Conducting marine traverses along the coastlines is hindered by severe weather conditions, a limited navigation and field work season, the absence of access roads, the presence of a border zone, and other factors.

Consequently, as of today, the northern part of the Schmidt Peninsula, the majority of the North Sakhalin Plain, the eastern coast of the island from Lunsky Bay to the village of Pogranichnoye, the Tym-Poronaysk Lowland and Terpeniya Peninsula, and the eastern coast of Krillion Peninsula remain poorly studied or unstudied.

Our field investigations yielded reliable data on various types of geological stress/strain indicators. Joints, without visible evidence of displacement, is the most widely represented. Less frequently observed are joints with mineralization in the form of crystals and druses, mineral crusts, as well as those lacking mineralization. Particular attention was paid to measurements of slickensides; tectonic stress reconstruction was primarily conducted based on these features, and accordingly, they constitute the foundation of the

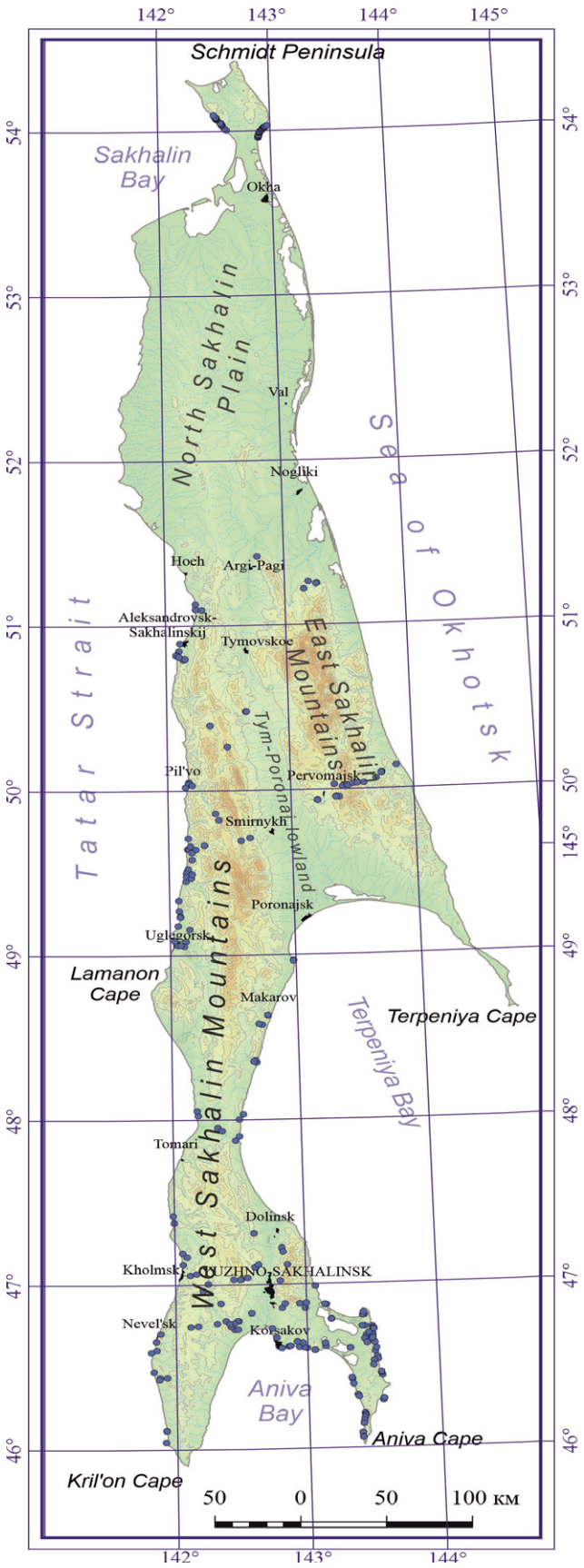

Map of the study area with the observation points.

Карта района исследования с нанесенными на нее точками наблюдения.

present work. In reconstructing stresses spatially associated with coal deposits in western Sakhalin, faults ranging from large-amplitude (displacement exceeding 1000 m) to fractures (less than 10 cm) were utilized. However, large-amplitude and medium-displacement (less than 10 m) faults, depicted on tectonic maps of areas with coal deposits, are most fully represented. These data were used for tectonophysical reconstruction, allowing for inference of the stress-strained state of the Earth's crust.

In some observation points, the replacement of certain geological stress indicators by other disjunctive features was recorded. This allowed for the identification of the relative sequence of structural formation.

Unfortunately, the scope of the present work precludes the detailed presentation of all available information. The majority of the research results have been published in our previous articles [3, 4, 7–10], with the corresponding level of detail. Full-scale and detailed results for all study areas are planned for regular posting on a dedicated page of the website of the Institute of Marine Geology and Geophysics of the Far Eastern Branch of the Russian Academy of Sciences.

As of today, the database of field tectonophysical investigations includes information for 264 observation points. An overview map, indicating these points, is presented below.

Methodology

The data utilized in this study were primarily obtained through the method of cataclastic analysis (MCA) of discontinuous displacements [5], as well as the structural-paragenetic method of analyzing minor disjunctive structures [15], O.I. Gushchenko's kinematic method [16], and M.V. Gzovsky's method of conjugate shear fractures [17]. Furthermore, L.A. Sim's method of generalizing – averaging – the stress field [18] was employed for the synthesis of field tectonophysical data. For processing field measurements of slickensides with established displacement kinematics, the method of cataclastic analysis [5] and the specifically developed STRESSgeol software [19], based on this method, were used. In addition, a modified algorithm of this method was also applied to process a series of measurements [20].

Quantitative and qualitative characteristics of the reconstructed local stress states were determined using the method of cataclastic analysis. The main characteristics include the angular orientation of the principal stress axes, as well as the magnitudes of the stresses themselves, the type of stress state, and the Lode–Nadai coefficient. The basic principles of the method of cataclastic analysis are based on the concepts of quasi-plastic deformation of the geological medium, as well as the tenets of plasticity theory under conditions of maximum dissipation of internal elastic energy for the calculated stress tensor. The STRESSgeol contains an automated algorithm for separating all data into homogeneous samples, which define the temporal phases of quasi-homogeneous deformation of the macrovolume, ensuring the maximum value of the total dissipation energy with the minimum number of identified phases. This method allows for a thorough examination of the stress-strained state of the Earth's crust.

The structural-paragenetic method of analysis of minor disjunctive structures by L.M. Rastsvetaev is based on the concept of quasi-plastic deformation of the rock mass. This concept ensures the energetic efficiency of displacements along previously formed discontinuities in the rock mass [15]. The method involves the use of the main types of geological stress indicators that describe the overall spatiotemporal series of quasi-plastic deformation of the studied area of rock. Minor disjunctive structures (tectonic fracturing) form certain template structural patterns that are interconnected by spatiotemporal characteristics and can be considered as paragenetic associations, or structural parageneses. Field data were synthesized in the form of structural diagrams and then analyzed both as individual points and

in a group manner in accordance with their place in the tectonic structure of the study area.

O.I. Gushchenko's kinematic method [16] is applied in processing field data on both the position of rupture planes and the orientation of slickensides. The method is based on the postulate of dislocation analysis, from which it follows that, with a known orientation of the principal stress axes, the direction of the displacement vector on the plane of an arbitrarily oriented fracture lies within the angle defined by the extreme values of the Lode–Nadai coefficient. The inverse problem of reconstructing the orientations of tectonic stresses that caused these displacements is solved based on the orientations of the displacement vectors on the ensemble of slickensides.

In M.V. Gzovsky's method of conjugate shear fractures, pairs of shear fractures – isochronous fractures that formed in a homogeneous stress field are selected. The conjugacy of shear fractures in two directions is determined by their merging, mutual intersection, or opposite directions of displacement [17]. The line of intersection of these fractures coincides with the axis of intermediate principal stress, and the bisectors of adjacent angles coincide with the directions of the principal stress axes.

Research results

From 2016 to 2023, a team of researchers conducted several short-term and long-term expeditions, including those for industrial purposes. Most of the results from these field investigations have been published [3, 4, 7–10]. Data systematization resulted in a summary of parameters characterizing the stress-strained state of the Earth's crust (calculated from field measurements) (see Tables 1 and 2 in the Appendix). Table 1 presents: the coordinates of observation points 1–212; the orientations of the principal stress axes (σ_1, minimum (extension), σ_2, intermediate, and σ_3, maximum (compression)), reconstructed using cataclastic analysis (MCA) based on structural-kinematic data from slickensides and joints; the type (environment) of the stress state; the Lode–Nadai coefficient (μ_σ); bedding planes; and the number of measurements at each point (total and those used for calculation in the STRESSgeol). Table 2 (from data in [4]) presents the available information on the principal stress axes. Data from [2, 3] reconstructing the principal stress axes using M.V. Gzovsky's method of conjugate shear fractures are also included.

Alongside other geological and geophysical data [21], the results presented in this study are integrated within a unified digital geoinformation system (GIS). Isoline GIS, provided by the developers for educational and research purposes, serves as our database management system. While primarily oriented towards the oil and gas and mining sectors [22], it provides a functional interface for working with the digital tectonophysical database. Simultaneous visualization and interpretation of diverse geological and geophysical information enables research at a new level. Furthermore, unlike results from past studies [2], this digital information is accessible to all interested researchers.

Investigations conducted from 2016 to 2023 revealed differences in the geodynamic setting between the eastern and western coasts of the Schmidt Peninsula. Horizontal shear regimes (shear type of deformation) predominate throughout this area. The western coast is characterized by a NW-trending orientation of the axis of maximum compression and its subhorizontal attitude. The eastern coast is characterized by horizontal extension regimes, typically localized in the axial parts of anticlinal structures. Directions of maximum compression are highly variable in this region. The parameters defining the stress-strained state of the Schmidt Peninsula differ significantly from those of the remainder of Sakhalin Island during the neotectonic period.

The central Sakhalin region exhibits a dominant subvertical orientation of the axis of maximum compression and a subhorizontal, most often submeridionally oriented axis of minimum compression (extension). Horizontal extension,

as a type of stress state, is characteristic of the entire central Sakhalin region. Horizontal compression and shear regimes are significantly more widespread in the western part of central Sakhalin. The number of horizontal extension regimes increases in the eastern and axial parts, approaching the Sea of Okhotsk.

Disruptive faults in the coal deposits of the western coast of Sakhalin Island are characterized by two, and less frequently three or four, density maxima on stereographic projections. Because most of the studied deposits are characterized by normal faults, fault elements whose bedding form each pair of maxima can be considered as conjugate.

A general pattern identified across all deposits is the nearly horizontal position of the extension axis, which is oriented sub-meridionally. A northerly to north-northeasterly trend of this axis is characteristic of the Lopatinskoe, Lesogorsk, Duysky, and Mgachi deposits, as well as a significant portion of the Uglegorsk and Boshnyakovo deposits; this abruptly changes to a sub-latitudinal trend in the southern Uglegorsk and Boshnyakovo deposits. The compression axis is oriented predominantly sub-latitudinally, with minor deviations in the southern and northern directions, and dip angles 30–70°.

Based on data from local stress states (LSS), the regional field of southern Sakhalin was reconstructed using the method of finding the "general", or averaged, field of tectonic stresses [18]. Two LSS were reconstructed in five homogeneously-axed volumes, and three LSS in one homogeneously-axed volume; the averaged stress field was determined using 36 local compression and extension axes. Their localization on a stereogram allowed determination of the compression and extension cones and the regional stress field with the following characteristics (defining the principal stress axes and allowing calculation of the Lode–Nadai coefficient, though those specifics were not measured in this case): σ_1 – 350° ∠10°; σ_2 – 112°∠66°; σ_3 – 260°∠20°; τ_{max} – (–32° ∠83°); τ_{max} – 125°∠68°.

Conclusion

This study provides a synthesis of key results from field tectonophysical investigations conducted during different years by various research groups at different times. The information on 264 observation points is presented in tabular format, containing crucial parameters of the stress-strained state of the Earth's crust in Sakhalin. In contrast to the outcomes of previous studies and analogous works in other regions, our database is fully integrated with a GIS and managed using the Isoline GIS software suite.

Thus, unique regional tectonophysical information has been combined, generalized, and systematized, making it possible to leverage this information for both fundamental and purely applied purposes, such as evaluating the stability of wellbores, quarry walls, slopes, and other engineering challenges. This enables a qualitatively new level of field tectonophysical investigations in conjunction with other geological and geophysical data. The database, which documents the orientation of slickensides and the distribution of fracturing, allowing the inference of principal stress axes and calculation of the Lode–Nadai coefficient, is continually updated with new results from field observations and will be made publicly available on a dedicated page of the website of the Institute of Marine Geology and Geophysics of the Far Eastern Branch of the Russian Academy of Sciences.

References

1. *Russian tectonophysics: In M.V. Gzovsky's 100th Anniversary commemoration*: Collectted works. **2019.** Apatity: FITS KNTS RAN, 359 p. (In Russ).
2. Shpetalenko L.P., Chmikhalova T.P., Chaynikova M.V. **1976.** [*Atlas of tectonic structures of Sakhalin coal deposits*]. Yuzhno-Sakhalinsk: Far East Publ. Hous, 93 p. (In Russ.).
3. Kamenev P.A., Marinin A.V. **2023.** Reconstruction of paleostresses in the West of Sakhalin from tectonophysical research findings. *Journal of Mining*

Science, 59(6): 919–929. https://doi.org/10.1134/S1062739123060054

4. Sim L.A., Bogomolov L.M., Bryantseva G.V., Savvichev P.A. **2017.** Neotectonics and tectonic stresses of the Sakhalin Island. *Geodynamics & Tectonophysics*, 8(1): 181–202. (In Russ.). https://doi.org/10.5800/GT-2017-8-1-0237
5. Rebetskiy Yu.L. **2007.** [*Tectonic stresses and strength of natural massifs*]. Moscow: Akademkniga, 406 p. (In Russ.).
6. Tataurova A.A. **2015.** Stress and strain fields based on data on crustal earthquake mechanisms in Sakhalin Island. *Vestnik KRAUNTs. Nauki o Zemle = Bull. of KRAESC. Earth Sciences*, 3(27): 93–101. (In Russ.).
7. Sim L.A., Bogomolov L.M., Kuchai O.A., Tataurova A.A. **2017.** Neotectonic and modern stresses of South Sakhalin. *Russian Journal of Pacific Geology*, 11(3): 223–235. https://doi.org/10.1134/s1819714017030058
8. Sim L.A., Kamenev P.A., Bogomolov L.M. **2020.** New data on the latest stress state of the earth's crust on Sakhalin Island (based on structural and geomorphological indicators of tectonic stress). *Geosistemy perehodnykh zon = Geosystems of Transition Zones*, 4(4): 372–383. (In Russ.). https://doi.org/10.30730/gtrz.2020.4.4.372-383
9. Marinin A.V., Rebetsky Yu.L, Sim L.A., Kamenev P.A., Kostrov Yu.V., Bondar I.V., Gordeev N.A., Degtyarev V.A. **2021.** Reconstruction of tectonic stresses on the Schmidt Peninsula, Sakhalin. *Vestnik KRAUNTs. Nauki o Zemle = Bull. of KRAESC. Earth Sciences*, 4(52): 73–88. (In Russ.). https://doi.org/10.31431/1816-5524-2021-4-52-73-88
10. Kamenev P.A., Marinin A.V., Degtyarev V.A., Lukmanov A.R. Reconstruction of tectonic stresses of the Central Sakhalin. **2023.** *Vestnik KRAUNTs. Nauki o Zemle = Bull. of KRAESC. Earth Sciences*, 57(1): 89–103. (In Russ.). https://doi.org/10.1134/s1819714023080079
11. Kamenev P.A., Marinin A.V. **2024.** *Sakhalin Island tectonophysical database*: certificate of registration of the database: RU 2024623290, No. 2024623016 of 12.07.2024; publ. 24.07.2024, Bull. № 8.
12. Sharueva L.I., Lopatin B.G., Roganov G.V. et al. (comp.) **2016.** [*State Geological map of Russian Federation on a scale of 1:1 000 000. Third generation. Far East series. Sheet N-54 (Nikolaevsk-na-Amure)*]: [Explanatory note]. Saint Petersburg: Kartograf. fabrika VSEGEI, 477 p. (In Russ.). URL: https://www.vsegei.ru/ru/info/pub_ggk1000-3/Dalnevostochnaya/n-54.php
13. Alenicheva A.A., Lizganov A.V., Ivanova V.V. et al. (comp.) **2019.** [*State Geological map of Russian Federation on a scale of 1:1 000 000. Third generation. Far East series. Sheet L-(53), 54 (Yuzhno-Sakhalinsk)*]: [Explanatory note]. St. Petersburg: Kartograf. fabrika VSEGEI, 536 p. (In Russ.). URL: https://www.vsegei.ru/ru/info/pub_ggk1000-3/Dalnevostochnaya/l-53-54.php
14. Richter A.V. **1986.** *The structure and tectonic development of Sakhalin in the Mesozoic*. Moscow: Nauka, 93 p. (Proceedings of the GIN RAS; Iss. 411). (In Russ.).
15. Rastsvetaev L.M. **1987.** Paragenetic method of structural analysis of disjunctive tectonic faults. In: *Problems of structural geology and physics of tectonic processes*. Moscow: GIN AN SSSR, pt. 2: 173–235. (In Russ.).
16. Gushchenko O.I. **1975.** The kinematic principle of reconstruction of the directions of the main stresses (according to geological and seismological data). *Doklady AN SSSR = Proceedings of the USSR Academy of Sciences*, 225(3): 557–560. (In Russ.).
17. Gzovsky M.V. **1975.** *Fundamentals of tectonophysics*. Moscow: Nauka, 535 p. (In Russ.).
18. Sim L.A. **1982**. [Determination of the regional field from the data on local stresses on separate sites]. *Izvestia vuzov. Geologiya i razvedka = Geology and Exploration*, 4: 35–40. (In Russ.).
19. Rebetskiy Yu.L., Sim L.A., Marinin A.V. **2017.** [*From slickensides to tectonic stresses. Methods and algorithms*]. Moscow: GEOS, 234 p. (In Russ.).
20. Rebetsky Yu.L., Sycheva N.A. **2024.** The stressed state of the Earth's crust in the Altai-Sayan mountain region: reconstruction based on the modified algorithms of the cataclastic method. *Geosistemy perehodnykh zon = Geosystems of Transition Zones*, 8(4): 261–276. (In Russ., abstr. in Engl.). https://doi.org/10.30730/gtrz.2024.8.4.261-276
21. Kamenev P.A., Degtyarev V.A., Zherdeva O.A., Kostrov Yu.V. **2024.** The fault kinematics of the Sakhalin Island based on geological and seismological methods. *Geosistemy perehodnykh zon = Geosystems of Transition Zones*, 8(1): 37–46; https://doi.org/10.30730/gtrz.2024.8.1.037-046, URL: http://journal.imgg.ru/web/full/f-e2024-1-3.pdf
22. Anisimov G.A., Valeeva S.E., Valeeva I.F., Anisimova L.Z. **2016.** About the current situation on the use of software systems in the mineral wealth use. *Exposition Oil & Gas*, 6(52): 13–15. (In Russ.).

APPENDIX / ПРИЛОЖЕНИЕ

Table 1. Parameters of the paleo-stress state in the area of the Sakhalin region (according to field research data of the authors and to published works during 1973–2023)

Таблица 1. Параметры палеонапряженного состояния территории о. Сахалин (по данным полевых исследований авторов и опубликованных источников за период с 1973 по 2023 г.)

No.	Observation point	Observation point coordinates		σ_1		σ_2		σ_3		Stress state type	μ_σ	Bedding planes	Measurements	
		N	E	Dip Az	∠	Dip Az	∠	Dip Az	∠				N total	N used
1	21108	46°23.321’	143°20.470’	83	24	338	30	205	50	Hor.Ext.	0.1	–	13	12
2	21109	46°25.637’	143°19.826’	277	30	164	34	38	42	Hor.Ext.	0.02	–	8	6
3	21110	46°25.079’	143°19.956’	214	12	308	19	95	67	Hor.Ext.	–0.12	–	9	5
4	21111	46°17.852’	143°34.045’	114	12	205	1	297	78	Hor.Ext.	0.02	–	10	10
5	21112	46°17.836’	143°34.106’	277	30	185	3	90	60	Hor.Ext.	0.02	–	12	12
6	21113	46°17.127’	143°33.961’	121	18	30	4	288	72	Hor.Ext.	0.35	–	12	9
7	22133	46°49.218’	143°25.845’	239	12	148	7	28	76	Hor.Ext.	0.04	259∠60	10	9
8	22134	46°44.459’	143°25.277’	165	19	73	6	326	71	Hor.Ext.	0.06		13	11
9	22135	46°52.702’	143°08.525’	112	34	202	1	293	56	Hor.Ext.	0.01	240∠30	11	9
10	22136	46°52.372’	143°09.315’	176	4	354	86	86	0	Hor.Sh.	–0.07	–	13	10
11	22152	46°43.158’	143°30.508’	90	0	360	12	180	78	Hor.Ext.	–0.01	335∠20	7	7
12	22153	46°43.342’	143°30.426’	342	25	251	4	153	65	Hor.Ext.	0.02	290∠25	10	6
13	22154	46°43.569’	143°30.097’	78	12	280	77	169	5	Hor.Sh	–0.05	80∠30	10	10
14	22155	46°44.309’	143°29.747’	139	11	232	16	16	71	Hor.Ext.	0.32	90∠70	9	9
15	22156	46°44.281’	143°26.445’	342	0	252	13	72	77	Hor.Ext.	0.01	–	10	10
16	22159	46°59.111’	143°04.332’	90	6	183	24	347	65	Hor.Ext.	–0.46	70∠15	11	10
17	22160	46°30.045’	143°29.843’	84	0	354	12	174	78	Hor.Ext.	0.6	–	11	8
18	22161	46°31.653’	143°30.340’	103	18	235	65	7	18	Hor.Sh	0.01	–	13	12
19	22162	46°32.122’	143°31.907’	283	18	191	4	90	72	Hor.Ext.	–0.05	–	13	11
20	22163	46°33.154’	143°31.851’	6	17	103	21	240	62	Hor.Ext.	0.27	–	10	6
21	22165	46°35.162’	143°30.798’	180	18	83	22	306	61	Hor.Ext.	0.13	–	10	10
22	22167	46°18.640’	143°22.765’	264	12	5	42	162	45	Hor.Ext.+Sh.	–0.33	–	8	7

No.	Observation point	Observation point coordinates		σ_1		σ_2		σ_3		Stress state type	μ_σ	Bedding planes	Measurements	
		N	E	Dip Az	∠	Dip Az	∠	Dip Az	∠				N total	N used
23	22168	46°19.306’	143°22.397’	90	36	203	28	321	41	Vert.Sh.	0.38	–	9	6
24	22185 A	46°03.941’	143°24.257’	246	6	337	8	120	80	Hor.Ext.	0.18	–	12	5
25	22185 B	46°03.941’	143°24.257’	276	0	6	86	186	4	Hor.Sh.	–0.3	–	12	7
26	22186	46°05.421’	143°24.012’	53	11	148	23	300	64	Hor.Ext.	–0.33	120∠70	12	10
27	22189	46°08.736’	143°24.552’	246	6	338	16	136	73	Hor.Ext.	–0.11	–	10	10
28	22190	46°09.966’	143°25.029’	308	17	126	73	218	1	Hor.Sh	–0.05	–	11	10
29	22191	46°11.048’	143°25.346’	202	21	107	13	346	65	Hor.Ext.	0	–	14	13
30	22192	46°11.714’	143°25.476’	248	34	7	36	129	36	Hor.Ext.+Sh.	–0.14	–	9	8
31	22193	46°12.124’	143°25.439’	292	34	37	21	153	48	Hor.Ext.	0.54	–	8	7
32	22194	46°12.722’	143°25.309’	284	29	188	11	79	58	Hor.Ext.	–0.24	–	9	9
33	22195	46°06.984’	141°55.250’	11	5	280	19	114	71	Hor.Ext.	0.02	–	8	8
34	22196	46°06.993’	141°55.315’	244	23	336	5	76	66	Hor.Ext.	–0.32	–	9	8
35	22197	46°02.751’	141°54.939’	153	63	275	15	11	22	Hor.Comp.	0	–	11	10
36	22206	46°38.473’	143°08.220’	308	17	206	34	59	51	Hor.Ext.	–0.33	–	10	8
37	22207	46°37.199’	143°08.306’	136	22	261	55	35	26	Hor.Sh.	0.29	–	14	13
38	23209	46°43.905’	142°44.130’	284	29	181	22	59	52	Hor.Ext.	–0.11	190∠20	10	9
39	23210	46°51.346’	142°49.002’	354	17	174	73	264	0	Hor.Sh.	–0.07	270∠20	12	12
40	23211	46°40.629’	142°45.948’	66	6	159	30	326	60	Hor.Ext.	–0.09	280∠10	10	10
41	23212	46°27.626’	143°33.337’	138	6	232	34	40	55	Hor.Ext.	–0.03	–	10	10
42	23213	46°27.372’	143°33.217’	250	23	153	17	30	61	Hor.Ext.	–0.24	–	8	7
43	23214	46°27.215’	143°33.289’	96	6	188	17	348	72	Hor.Ext.	–0.05	–	8	8
44	23215	46°26.351’	143°33.911’	318	6	227	9	80	80	Hor.Ext.	0.21	–	8	7
45	23216 A	46°47.125’	143°11.403’	174	29	54	42	286	34	Hor.Sh.	0.26	–	9	4
46	23216 B	46°47.125’	143°11.403’	264	6	171	23	8	66	Hor.Ext.	–0.31	–	9	4
47	23218	46°35.872’	143°03.362’	6	0	276	12	96	78	Hor.Ext.	–0.32	–	12	12

No.	Observation point	Observation point coordinates		σ_1		σ_2		σ_3		Stress state type	μ_σ	Bedding planes	Measurements	
		N	E	Dip Az	∠	Dip Az	∠	Dip Az	∠				N total	N used
48	23219 A	46°35.937’	143°03.449’	66	40	325	13	220	47	Vert.Sh.	0.56	–	11	7
49	23219 B	46°35.937’	143°03.449’	18	0	108	0	270	90	Hor.Ext.	0.14	–	11	4
50	23220 A	46°36.521’	143°19.384’	264	12	161	46	5	42	Hor.Ext.+Sh.	0.02	–	16	6
51	23220 B	46°36.521’	143°19.384’	24	0	114	0	270	90	Hor.Ext.	0.13	–	16	10
52	23221	46°41.937’	143°28.174’	341	15	247	14	115	69	Hor.Ext.	0.51	–	10	10
53	23222 A	46°39.869’	143°29.928’	249	28	344	9	90	60	Hor.Ext.	–0.05	–	8	3
54	23222 B	46°39.869’	143°29.928’	146	36	237	1	328	54	Vert.Sh.	–0.41	–	8	5
55	23223	46°40.926’	143°29.763’	264	12	359	25	150	62	Hor.Ext.	0.35	–	10	7
56	23224	46°41.290’	143°29.841’	42	0	132	0	270	90	Hor.Ext.	–0.04	–	7	7
57	23225	46°41.815’	143°28.462’	323	21	213	41	73	41	Hor.Ext.+Sh.	–0.36	–	8	8
58	23226	46°48.437’	143°25.712’	211	30	318	27	81	48	Hor.Ext.	0.03	210∠60	11	9
59	23227	46°48.655’	143°26.544’	108	11	206	33	2	54	Hor.Ext.	0.17	260∠40	10	10
60	23228	46°36.778’	142°58.918’	257	23	129	55	358	25	Hor.Sh	0.03	–	10	10
61	23229	46°37.091’	142°56.477’	252	11	156	28	2	60	Hor.Ext.	–0.04	260∠40	12	12
62	23230	46°36.591’	142°59.978’	288	47	142	38	38	18	Hor.Comp.+Sh.	0.47	–	8	7
63	23231	46°37.507’	142°52.332’	114	6	205	11	356	78	Hor.Ext.	0.13	–	10	10
64	23232	46°37.411’	142°52.006’	90	36	360	0	270	54	Vert.Sh.	–0.05	–	7	6
65	23233	46°37.361’	142°51.462’	115	12	213	34	8	53	Hor.Ext.	–0.39	–	7	7
66	20060	50°05.563’	143°44.308’	167	27	66	21	304	54	Hor.Ext.	0.04	329∠10	8	8
67	20061	50°05.644’	143°44.541’	146	26	54	4	317	64	Hor.Ext.	0.42	334∠10	9	9
68	20062	50°05.724’	143°44.634’	131	27	232	19	353	55	Hor.Ext.	–0.01	284∠12	7	7
69	20066	50°08.174’	143°51.883’	349	21	246	29	110	52	Hor.Ext.	–0.01	214∠50	8	8
70	20068	50°03.654’	143°41.660’	202	10	72	74	294	12	Hor.Sh	0.01	204∠10	7	5
71	20072	46°28.449’	141°49.797’	180	12	280	41	77	47	Hor.Ext.+Sh.	0.11	64∠30	6	5
72	20073	46°35.385’	141°48.781’	258	12	348	2	90	78	Hor.Ext.	–0.05	–	10	10

No.	Observation point	Observation point coordinates		σ_1		σ_2		σ_3		Stress state type	μ_σ	Bedding planes	Measurements	
		N	E	Dip Az	∠	Dip Az	∠	Dip Az	∠				N total	N used
73	20074	46°36.318’	141°51.125’	126	6	33	28	226	61	Hor.Ext.	–0.13	–	9	4
74	21075	48°21.340’	142°38.755’	108	6	6	65	201	24	Hor.Sh	–0.03	79∠70	14	13
75	21076	48°21.861’	142°39.490’	258	6	167	10	17	78	Hor.Ext.	0.03	109∠70	12	9
76	21077	48°35.008’	142°41.559’	276	0	6	18	186	72	Hor.Ext.	0.11	89∠75	6	4
77	21078	48°34.602’	142°43.104’	216	6	316	60	122	29	Hor.Sh	0.08	79∠70	12	10
78	21079	48°38.185’	142°45.962’	245	18	153	5	46	71	Hor.Ext.	0.16	–	11	8
79	21080	48°38.089’	142°45.920’	110	23	16	7	270	66	Hor.Ext.	0.08	–	12	12
80	21081	48°20.857’	142°39.987’	102	12	196	16	337	70	Hor.Ext.	–0.37	–	8	7
81	21083	49°14.159’	142°05.091’	288	11	21	15	162	71	Hor.Ext.	0.13	–	10	8
82	21084	49°14.211’	142°05.106’	251	17	136	54	351	30	Hor.Sh	0.14	–	10	5
83	21086	49°38.715’	142°09.828’	78	0	168	50	348	40	Hor.Ext.+Sh.	–0.3	71∠80	10	8
84	21087	49°38.802’	142°09.305’	203	5	112	16	311	74	Hor.Ext.	–0.45	–	8	7
85	21088	49°29.997’	142°08.493’	318	5	226	26	59	64	Hor.Ext.	0.01	–	9	6
86	21089	49°26.968’	142°08.192’	205	16	301	18	76	65	Hor.Ext.	0.29	–	11	9
87	21091	49°16.268’	142°04.580’	188	8	287	46	91	42	Hor.Ext.+Sh.	–0.1	–	8	6
88	21092	49°10.866’	142°04.018’	258	12	167	3	62	78	Hor.Ext.	0.1	224∠15	10	10
89	21093	50°47.927’	142°09.546’	69.4	28.4	335	8	231	60	Hor.Ext.	0.03	–	8	8
90	21094	50°47.597’	142°08.744’	356	4	264	24	95	66	Hor.Ext.	0.23	–	8	8
91	21095	50°49.300’	142°05.214’	83.1	29.8	345.8	12.5	235.7	57.2	Hor.Ext.	0.38	–	13	10
92	21096	50°49.370’	142°05.416’	348	28	127	56	247	19	Hor.Sh	–0.09	–	9	5
93	21097	50°50.872’	142°06.647’	306	6	48	63	214	26	Hor.Sh	0.18	–	15	10
94	21098	50°53.579’	142°07.202’	77	18	169	4	270	72	Hor.Ext.	–0.39	265∠80	12	6
95	21099	51°06.044’	142°15.267’	294	0	24	41	204	49	Hor.Ext.+Sh.	–0.24	–	9	9
96	21100	51°14.853’	143°15.854’	306	6	216	4	94	83	Hor.Ext.	–0.05	250∠45	10	7
97	21101	51°15.078’	143°15.927’	252	6	157	42	348	48	Hor.Ext.+Sh.	0.28	–	10	8

No.	Observation point	Observation point coordinates		σ_1		σ_2		σ_3		Stress state type	μ_σ	Bedding planes	Measurements	
		N	E	Dip Az	∠	Dip Az	∠	Dip Az	∠				N total	N used
98	21102	51°15.576’	143°11.999’	180	60	312	21	50	20	Hor.Comp.	–0.41	–	8	5
99	21103	51°13.150’	143°09.459’	282	0	192	31	12	59	Hor.Ext.	0.07	–	12	11
100	21104	51°25.073’	142°46.674’	142	42	7	38	256	24	Hor.Ext.+Sh.	–0.05	–	10	7
101	21106	50°28.733’	142°39.080’	62	63	193	18	290	19	Hor.Comp.	0.05	–	10	7
102	21107	50°28.692’	142°39.084’	229	27	48	63	138	0	Hor.Sh	–0.13	–	8	8
103	21114	50°02.152’	143°35.603’	185	11	90	24	298	63	Hor.Ext.	–0.07	–	11	10
104	21115	50°02.067’	143°32.357’	120	6	214	32	21	57	Hor.Ext.	–0.24	239∠40	13	12
105	21116	50°01.909’	143°30.383’	216	6	306	5	75	82	Hor.Ext.	0.12	–	9	9
106	21117	50°01.245’	143°28.148’	199	15	293	14	65	69	Hor.Ext.	0.3	229∠60	10	10
107	21118	50°01.336’	143°27.169’	289	71	158	13	65	14	Hor.Comp.	–0.48	–	10	9
108	21119	50°00.951’	143°25.257’	47	11	138	4	246	78	Hor.Ext.	–0.06	–	10	10
109	21120	49°57.087’	143°21.995’	161	15	264	40	55	46	Hor.Ext.+Sh.	0.28	–	11	7
110	21121	49°57.153’	143°23.389’	206	16	299	13	66	69	Hor.Ext.	0.05	–	11	8
111	21122	49°57.249’	143°22.181’	282	12	192	2	90	78	Hor.Ext.	–0.08	–	9	8
112	21123	50°01.715’	143°21.344’	162	25	71	4	333	65	Hor.Ext.	0.04	–	9	7
113	21124	50°01.715’	143°21.344’	270	12	7	29	160	58	Hor.Ext.	0.33	–	8	8
114	21125	48°57.868’	142°58.690’	36	6	300	44	132	46	Hor.Ext.+Sh.	–0.13	220∠20	11	9
115	21126	48°58.014’	142°58.714’	110	23	19	2	284	67	Hor.Ext.	0.27	–	9	7
116	22129	47°52.498’	142°29.129’	66	6	334	16	175	73	Hor.Ext.	0.32	–	14	11
117	22130	47°07.371’	142°03.787’	276	18	173	36	28	49	Hor.Ext.+Sh.	–0.16	–	7	5
118	22131	47°10.191’	142°05.535’	9	9	260	65	102	24	Hor.Sh	–0.05	15∠30	7	7
119	22137	46°25.564’	141°52.433’	48	0	138	45	318	46	Hor.Ext.+Sh.	–0.27	90∠15	14	10
120	22138	46°26.270’	141°52.603’	336	0	246	72	66	18	Hor.Sh	0.1	98∠15	13	13
121	22139	46°26.161’	141°56.009’	174	23	268	8	14	65	Hor.Ext.	0.2	240∠85	11	11
122	22140	47°02.456’	142°33.479’	60	6	329	5	199	82	Hor.Ext.	–0.01	–	15	11

No.	Observation point	Observation point coordinates		σ_1		σ_2		σ_3		Stress state type	μ_σ	Bedding planes	Measurements	
		N	E	Dip Az	∠	Dip Az	∠	Dip Az	∠				N total	N used
123	22140-2	47°01.825’	142°27.015’	200	31	98	19	341	53	Hor.Ext.	0.21	–	14	7
124	22141	47°01.872’	142°30.020’	4	4	270	42	99	48	Hor.Ext.+Sh.	0.19	300∠10	13	9
125	22142	47°02.019’	142°30.645’	338	10	237	48	77	40	Hor.Ext.+Sh.	–0.08	75∠20	6	5
126	22144	49°34.865’	142°11.18’	152	11	46	54	249	34	Hor.Sh	0.18	219∠80	12	7
127	22145	49°09.477’	142°09.486’	270	72	121	16	29	9	Hor.Comp.	–0.12	–	12	10
128	22146	49°40.071’	142°17.286’	338	21	79	26	215	56	Hor.Ext.	–0.34	–	14	12
129	22147	49°42.623’	142°09.451’	195	11	46	78	286	6	Hor.Sh	–0.13	–	15	14
130	22148	49°31.386’	142°09.158’	283	18	15	8	127	71	Hor.Ext.	–0.52	–	13	11
131	22149	49°31.026’	142°08.947’	283	18	191	4	90	72	Hor.Ext.	0.14	–	9	6
132	22150	49°20.126’	142°04.568’	11	5	260	77	102	12	Hor.Sh	–0.36	–	8	6
133	22157	47°00.187’	142°15.088’	31	30	296	8	192	58	Hor.Ext.	0.01	215∠10	11	11
134	22158	46°57.909’	142°12.941’	120	6	210	2	320	84	Hor.Ext.	0.16	110∠50	7	7
135	22170	49°42.631’	142°39.657’	60	6	156	47	324	42	Hor.Ext.+Sh.	–0.49	340∠25	12	7
136	22171	49°41.584’	142°35.139’	157	5	249	27	56	63	Hor.Ext.	0.35	290∠60	8	8
137	22172	49°49.256’	142°24.513’	284	29	150	51	28	23	Hor.Sh	–0.17	250∠70	12	12
138	22173	50°01.859’	142°11.819’	360	6	91	12	244	77	Hor.Ext.	0.1	70∠75	13	12
139	22174	50°01.209’	142°08.554’	11	5	109	60	279	30	Hor.Sh	–0.11	–	10	9
140	22175	50°02.437’	142°10.063’	47	11	309	34	152	53	Hor.Ext.	0.1	–	10	10
141	22176	50°02.822’	142°10.643’	285	65	102	25	192	1	Hor.Comp.	0.01	–	12	12
142	22177	50°03.076’	142°10.297’	186	17	92	13	327	69	Hor.Ext.	0	–	11	10
143	22178	49°51.517’	142°22.917’	187	42	285	9	25	47	Vert.Sh.	0.11	–	8	8
144	22179	50°15.851’	142°29.559’	355	11	87	7	207	77	Hor.Ext.	–0.02	80∠85	12	11
145	22182	50°23.681’	142°21.155’	310	51	70	22	174	30	Hor.Comp.	0.02	255∠75	8	8
146	22183	49°56.017’	143°12.834’	360	6	262	53	94	36	Hor.Ext.+Sh.	0.01	–	11	11
147	22184	49°56.036’	143°12.817’	68	34	309	36	187	36	Hor.Ext.+Sh.	–0.03	–	9	8

No.	Observation point	Observation point coordinates		σ_1		σ_2		σ_3		Stress state type	μ_σ	Bedding planes	Measurements	
		N	E	Dip Az	∠	Dip Az	∠	Dip Az	∠				N total	N used
148	22205	50°28.754’	142°38.860’	111	28	215	25	340	50	Hor.Ext.	0.06	–	10	7
149	20277	54°05.702’	142°30.041’	42	37	209	52	307	7	Hor.Comp.+Sh.	0.1	–	11	10
150	20769	54°04.954’	142°31.011’	185	11	80	52	283	36	Hor.Ext.+Sh.	0.18	248∠62	16	10
151	20272m	54°04.894’	142°31.093’	255	35	72	55	164	2	Hor.Sh	0.22	248∠60	6	4
152	20272g	54°04.887’	142°31.079’	36	0	126	73	306	17	Hor.Sh	–0.05	–	15	10
153	20767m	54°04.879’	142°31.106’	231	22	355	54	129	26	Hor.Sh	–0.56	258∠50	11	10
154	20767k	54°04.879’	142°31.106’	270	42	56	43	163	18	Hor.Ext.+Sh.	–0.08	258∠50	12	10
155	20766m	54°04.856’	142°31.123’	277	30	122	58	13	11	Hor.Sh	–0.22	248∠55	12	11
156	20766k	54°04.856’	142°31.123’	54	6	321	27	155	63	Hor.Ext.	–0.03	248∠55	8	8
157	20279	54°04.787’	142°31.196’	171	53	44	24	302	26	Hor.Comp.	0.41	300∠0	13	6
158	20281	54°04.728’	142°31.236’	210	6	306	50	115	40	Hor.Ext.+Sh.	0.14	240∠44	7	4
159	20280	54°04.718’	142°31.250’	231	22	24	66	137	10	Hor.Sh	0.35	230∠56	7	5
160	20771	54°04.699’	142°31.240’	212	17	357	69	119	11	Hor.Sh	0.21	235∠44	14	11
161	20278	54°04.695’	142°31.241’	202	21	39	68	294	6	Hor.Sh	0.29	228∠51	4	3
162	20812	54°04.672’	142°31.273’	288	6	21	30	189	59	Hor.Ext.	–0.39	228∠40	8	7
163	20282	54°04.666’	142°31.280’	62	29	201	54	321	20	Hor.Sh	0.12	–	9	6
164	20773	54°04.625’	142°31.301’	31	30	200	59	298	5	Hor.Sh	0.15	243∠46	10	10
165	20774	54°04.505’	142°31.397’	68	34	246	56	338	1	Hor.Sh	–0.24	248∠50	6	6
166	20775	54°04.364’	142°31.505’	186	17	6	73	276	0	Hor.Sh	–0.12	238∠60	16	10
167	20287	54°04.061’	142°31.775’	26	77	230	12	138	5	Hor.Comp.	–0.5	–	7	5
168	20292	54°02.955’	142°33.447’	174	17	268	13	33	69	Hor.Ext.	0.46	245∠35	5	3
169	20291	54°02.931’	142°33.476’	315	82	210	2	120	8	Hor.Comp.	0.22	–	11	9
170	20782	54°02.927’	142°33.474’	270	90	234	0	324	0	Hor.Comp.	0.06	240∠21	24	20
171	20293k	54°02.800’	142°33.700’	44	66	249	32	152	0	Hor.Comp.	–0.13	–	11	9
172	20293g	54°02.801’	142°33.690’	90	78	348	3	258	0	Hor.Comp.	–0.19	239∠21	10	10

No.	Observation point	Observation point coordinates		σ_1		σ_2		σ_3		Stress state type	μ_σ	Bedding planes	Measurements	
		N	E	Dip Az	∠	Dip Az	∠	Dip Az	∠				N total	N used
173	20294	54°02.359’	142°34.245’	109	71	228	10	321	0	Hor.Comp.	0.18	230∠23	17	11
174	20295	54°02.224’	142°34.286’	233	11	27	78	142	0	Hor.Sh	–0.05	233∠33	7	6
175	20784	54°02.009’	142°34.399’	307	11	216	2	115	0	Hor.Ext.	–0.21	238∠35	12	10
176	20297	54°01.988’	142°34.417’	262	42	49	43	156	0	Hor.Comp.+Sh.	–0.12	216∠26	12	7
177	20785	54°01.935’	142°34.455’	338	57	209	22	109	0	Hor.Comp.	0.14	233∠38	12	11
178	20789	54°00.980’	142°35.641’	90	36	270	54	0	0	Hor.Comp.+Sh.	0.38	–	5	4
179	20791	54°00.211’	142°36.772’	270	48	74	41	171	0	Hor.Comp.+Sh.	0.17	198∠30	5	4
180	20816m	54°01.818’	142°58.375’	300	6	34	32	201	57	Hor.Ext.	–0.46	–	9	9
181	20816b	54°01.818’	142°58.375’	141	16	273	67	46	17	Hor.Sh,	0.2	–	18	11
182	20819 и 20820	54°01.450’	142°57.457’	264	12	66	78	173	4	Hor.Sh,	–0.15	68∠48	11	8
183	20821	54°01.328’	142°57.270’	108	6	15	27	209	63	Hor.Ext.	–0.03	13∠40	11	8
184	20822	54°01.217’	142°57.155’	206	77	310	3	41	13	Hor.Comp.	0.12	228∠60	12	8
185	20823 и 20824	54°01.170’	142°57.023’	209	22	103	35	325	47	Hor.Ext.	–0.25	128∠45	7	5
186	20326	54°01.058’	142°56.815’	189	9	92	36	290	52	Hor.Ext.+Sh.	0.25	–	14	10
187	20327	54°01.015’	142°56.746’	218	42	18	47	119	10	Hor.Comp.+Sh.	0.25	313∠25	9	5
188	20328	54°00.955’	142°56.551’	138	37	3	43	248	25	Hor.Comp.+Sh.	0.11	218∠37	13	6
189	20330	54°00.541’	142°56.117’	233	11	54	79	323	0	Hor.Sh	–0.1	58∠61	12	10
190	20331	54°00.514’	142°56.136’	246	6	153	3	346	60	Hor.Ext.	–0.18	28∠75	16	15
191	20826	54°00.505’	142°56.089’	240	35	46	54	146	7	Hor.Sh	0.05	203∠55	24	13
192	20827	54°00.485’	142°56.048’	0	0	270	90	90	0	Hor.Sh	0.18	63∠35	10	5
193	20830	54°00.427’	142°55.879’	270	72	53	15	145	11	Hor.Comp.	0.45	38∠35	9	4
194	20831	54°00.364’	142°55.745’	233	11	140	14	0	72	Hor.Ext.	–0.07	118∠24	13	11
195	20832	54°00.140’	142°55.535’	262	42	49	43	156	17	Hor.Comp.+Sh.	0.11	178∠25	14	12
196	20835	53°59.897’	142°55.006’	279	48	76	40	176	12	Hor.Comp.+Sh.	–0.32	243∠52	16	14

No.	Observation point	Observation point coordinates		σ_1		σ_2		σ_3		Stress state type	μ_σ	Bedding planes	Measurements	
		N	E	Dip Az	∠	Dip Az	∠	Dip Az	∠				N total	N used
197	20337	53°59.891’	142°55.004’	41	11	297	51	139	37	Hor.Ext.+Sh.	0.08	59∠57	9	8
198	20341	53°59.542’	142°54.595’	64	23	164	22	292	57	Hor.Ext.	–0.27	–	10	9
199	20342	53°59.475’	142°54.515’	249	28	137	36	8	41	Hor.Ext.+Sh.	–0.12	100∠26	10	6
200	20838	53°59.424’	142°54.467’	60	0	330	50	150	40	Hor.Ext.+Sh.	–0.04	48∠75	8	5
201	20842	53°59.281’	142°54.385’	246	6	343	49	151	40	Hor.Ext.+Sh.	0.1	38∠70	6	6
202	20843	53°59.250’	142°54.362’	38	42	131	3	225	48	Vert.Sh.	–0.42	62∠60	11	7
203	20841	53°59.108’	142°54.257’	66	6	157	10	307	78	Hor.Ext.	–0.07	218∠52	11	9
204	20345	53°59.095’	142°54.268’	108	6	215	71	16	19	Hor.Sh.	0.12	70∠75	10	7
205	20846	53°58.354’	142°53.879’	257	18	134	60	355	23	Hor.Sh.	0.14	208∠55	12	8
206	20847	53°58.141’	142°53.810’	206	49	73	31	327	24	Hor.Comp.	–0.27	–	7	5
207	20809k	53°58.104’	142°53.797’	51	22	171	51	307	30	Hor.Sh.	0.43	33∠45	11	7
208	20809g	53°58.104’	142°53.797’	270	24	104	65	358	8	Hor.Sh.	–0.13	53∠33	7	6
209	20809b	53°58.104’	142°53.797’	47	11	202	78	316	5	Hor.Sh.	0.45	28∠42	5	4
210	20807	53°57.629’	142°53.617’	157	5	66	6	290	82	Hor.Ext.	0.06	–	14	11
211	20806	53°57.606’	142°53.601’	123	24	18	31	244	49	Hor.Ext.	0.29	249∠76	12	7
212	20805	53°57.575’	142°53.596’	52	17	166	53	312	32	Hor.Sh.	–0.31	258∠50	11	7

Notes. The table shows the number and coordinates of the observation points; the orientation of the principal stress axes (σ_1, minimum (extension); σ_2, intermediate; σ_3, maximum compressive stresses) reconstructed using the cataclastic method [5] according to structural and kinematic data on the slickensides and joints; type of the stress state (Hor.Ext., horizontal extension; Hor.Ext.+Sh., horizontal extension with shear; Hor.Sh., horizontal shear; Hor.Comp., horizontal compression; Hor.Comp.+Sh., horizontal compression with shear; Vert.Sh., vertical shear); the Lode–Nadai coefficient μ_σ; betting plane dip; the total number of measurements at the point and used for calculation in the STRESSgeol software. Dash denotes that no data available.

Примечания. В таблице приведены номер и координаты точек наблюдения; ориентировки осей главных напряжений (σ_1 – минимальных (растяжение), σ_2 – промежуточных и σ_3 – максимальных сжимающих напряжений), реконструированные при помощи катакластического метода [5] по структурно-кинематическим данным о зеркалах скольжения и трещинах; тип (обстановка) напряженного состояния (Hor.Ext. – горизонтальное растяжение, Hor.Ext.+Sh. – горизонтальное растяжение в сочетании со сдвигом, Hor.Sh. – горизонтальный сдвиг, Hor.Comp. – горизонтальное сжатие, Hor.Comp.+Sh. – горизонтальное сжатие в сочетании со сдвигом, Vert.Sh. – сдвиг в вертикальной плоскости); коэффициент Лоде–Надаи μ_σ; элементы залегания слоистости; общее количество замеров в точке и использованных для расчета в программе STRESSgeol. Прочерк – данные отсутствуют.

Table 2. Information on orientation of principal stress axes for observation points No. 213–264 (according to [2–4, 7, 8])
Таблица 2. Сведения об ориентировке осей главных напряжений для точек наблюдения 213–264 (по данным [2–4, 7, 8])

No.	Observation point	Coordinates or location of observation point		σ_1		σ_2		σ_3	
		N	E	Dip Az	∠	Dip Az	∠	Dip Az	∠
213	1	47°01.450’	142°48.217’	6	20	106	25	243	56
214	2a	46°39.483’	141°50.950’	202	20	356	67	110	9
215	2b	Nevelsk, northern suburb and southern part of marine terrace		356	67	202	20	108	10
216	3	46°44.667’	142°07.017’	162	30	21	55	264	18
217	4	46°51.133’	142°59.500’	34	10	130	32	288	54
218	5	Lyutoga River, near the bridge up of the village of Ogon’ki		18	10	271	68	112	20
219	6a	46°46.800’	142°28.433’	176	36	65	28	306	40
220	6b	Center of the quarry near the settlement of Petropavlovskoe, old field		65	30	176	32	302	43
221	7	The entrance to the Petropavlovskiy quarry		330	50	196	30	90	20
222	8	46°37.033’	142°58.133’	132	23	343	65	227	10
223	9	Mt. Yunona		208	10	345	75	118	10
224	10	Town of Korsakov, rocky wall		314	30	176	52	58	30
225	11	48°00.167’	142°31.250’	210	5	116	50	304	40
226	12a	47°06.220’	142°36.910’	320	40	228	2	134	50
227	12b	The left bank of the Susuya river to the south of the Sanatorny village		159	35	35	38	274	30
228	13	46°40.973’	143°27.212’	82	10	218	74	348	10
229	14a	46°38.278’	143°30.705’	347	30	182	56	80	5
230	14b	Cape Ptichiy by the Sea of Okhotsk		322	20	64	26	195	55
231	14c	Cape Ptichiy by the Sea of Okhotsk		20	20	150	60	280	20
232	15	46°39.353’	143°28.685’	152	10	246	18	34	68
233	16	46°46.743’	142°28.975’	188	5	293	64	97	24
234	17a	The left bank of the river Tsunai under the bridge on the highway Yuzhno-Sakhalinsk–Kholmsk		16	15	116	26	254	56

No.	Observation point	Coordinates or location of observation point		σ_1		σ_2		σ_3	
		N	E	Dip Az	∠	Dip Az	∠	Dip Az	∠
235	18	47°22.585’	141°59.883’	152	30	20	50	255	26
236	19	The shore of the Tatar Strait, Simakovo village, cut into the road		318	10	54	21	204	61
237	20	47°03.502’	142°07.025’	52	15	322	0	237	70
238	21a	Yuzhno-Sokolovsky quarry, young field		256	70	40	18	132	12
239	21b	Yuzhno-Sokolovsky quarry, old field		42	18	260	70	130	12
240	22	Yuzhno-Sokolovsky quarry, foot wall of the fault		268	70	130	12	36	10
241	23	Ilyinsky village, the left bank of the Jasminka river		319	30	104	53	216	18
242	24	Ilyinsky village, right bank of the Jasminka river		206	25	94	40	320	40
243	25	47°57.230’	142°20.988’	306	3	216	74	38	14
244	26	Northern outskirts of the village of Vzmorye		234	60	26	16	122	10
245	27	46°43.600’	142°26.917’	145	10	297	76	53	5
246	28a	46°53.133’	142°20.988’	155	20	359	56	250	10
247	28b	Izvestkovy quarry, old field		92	42	194	14	300	45
248	29	Izvestkovy quarry, eastern wall		144	47	3	35	256	20
249	Due deposit			195	5	100	60	295	60
250	Lopatinskoe deposit (Dolinskaya mine)			215	5	315	25	120	30
251	Mgachi deposit (west wing)			215	5	125	60	305	30
252	Mgachi deposit (east wing)			0	5	270	60	90	35
253	Boshnyakovo deposit (west wing)			240	20	45	70	150	10
254	Boshnyakovo deposit (east wing)			5	5	275	60	100	25
255	Boshnyakovo deposit (southern centroclinal)			270	5	175	70	5	20
256	Boshnyakovo deposit (northern centroclinal)			25	10	290	5	150	80
257	Lesogorsk deposit (Telnovskaya mine)			335	10	65	20	225	70
258	Lesogorsk deposit (Upper Telnovskaya 1)			20	5	280	25	110	25
259	Lesogorsk deposit (Upper Telnovskaya 2)			225	5	315	15	130	70
260	Uglegorsk deposit (Sergeevsky site)			180	30	20	40	280	5

No.	Observation point	Coordinates or location of observation point		σ_1		σ_2		σ_3	
		N	E	Dip Az	∠	Dip Az	∠	Dip Az	∠
261	Uglegorsk deposit (Uglegorsk 6 mine)			150	5	240	40	50	55
262	Uglegorsk deposit (Uglegorsk 4-1 mine)			320	20	220	30	75	50
263	Uglegorsk deposit (Uglegorsk 4-2 mine)			220	50	40	40	130	0
264	Uglegorsk deposit (Udarnovskaya mine)			240	50	25	30	125	20

Note. The orientation of the principal stress axes: σ_1, minimum (extension); σ_2, intermediate; σ_3, maximum compressive stresses.

Примечание. Ориентировка осей главных напряжений: σ_1 – минимальных (растяжение), σ_2 – промежуточных и σ_3 – максимальных сжимающих напряжений.

About the Authors

Kamenev, Pavel A. (https://orcid.org/0000-0002-9934-5855), Cand. Sci. (Engineering), Senior Researcher, Laboratory of geochemistry and regional geology, Institute of Marine Geology and Geophysics of the Far Eastern Branch of RAS, Yuzhno-Sakhalinsk, Russia, p.kamenev@imgg.ru

Marinin, Anton V. (https://orcid.org/0000-0002-1099-6492), Cand. Sci. (Geology and Mineralogy), Lead Researcher, Laboratory fundamental and applied problems of tectonophysics, Schmidt Institute of Physics of the Earth of the Russian Academy of Sciences, Moscow, Russia, marinin@ifz.ru

Sim, Lydia A. (https://orcid.org/0000-0003-0267-2241), Doctor of Geology and Mineralogy, Lead Researcher, Laboratory of fundamental and applied problems of tectonophysics, Schmidt Institute of Physics of the Earth of the Russian Academy of Sciences, Moscow, Russia, sim@ifz.ru

Bogomolov, Leonid M. (https://orcid.org/0000-0002-9124-9797), Doctor of Physics and Mathematics, Director, Institute of Marine Geology and Geophysics of the Far Eastern Branch of RAS, Yuzhno-Sakhalinsk, Russia, bleom@mail.ru

Lukmanov, Anton R., Researcher, Laboratory fundamental and applied problems of tectonophysics, Schmidt Institute of Physics of the Earth of the Russian Academy of Sciences, Moscow, Russia, antonlukmanov@mail.ru

Degtyarev, Vladislav A. (https://orcid.org/0000-0001-8922-3654), Researcher, Laboratory of geochemistry and regional geology, Institute of Marine Geology and Geophysics of the Far Eastern Branch of RAS, Yuzhno-Sakhalinsk, Russia, degtyarevvladislav96@yandex.ru

Об авторах

Каменев Павел Александрович (https://orcid.org/0000-0002-9934-5855), кандидат технических наук, старший научный сотрудник лаборатории геохимии и региональной геологии, Институт морской геологии и геофизики Дальневосточного отделения РАН, Южно-Сахалинск, Россия, p.kamenev@imgg.ru

Маринин Антон Витальевич (https://orcid.org/0000-0002-1099-6492), кандидат геолого-минералогических наук, ведущий научный сотрудник лаборатории фундаментальных и прикладных проблем тектонофизики, Институт физики Земли им. О.Ю. Шмидта РАН, Москва, Россия, marinin@ifz.ru

Сим Лидия Андреевна (https://orcid.org/0000-0003-0267-2241), доктор геолого-минералогических наук, ведущий научный сотрудник лаборатории фундаментальных и прикладных проблем тектонофизики, Институт физики Земли им. О.Ю. Шмидта РАН, Москва, Россия, sim@ifz.ru

Богомолов Леонид Михайлович (https://orcid.org/0000-0002-9124-9797), доктор физико-математических наук, директор, Институт морской геологии и геофизики ДВО РАН, Южно-Сахалинск, Россия, bleom@mail.ru

Лукманов Антон Романович, научный сотрудник лаборатории фундаментальных и прикладных проблем тектонофизики, Институт физики Земли им. О.Ю. Шмидта РАН, Москва, Россия, antonlukmanov@mail.ru

Дегтярев Владислав Анатольевич (https://orcid.org/0000-0001-8922-3654), научный сотрудник лаборатории геохимии и региональной геологии, Институт морской геологии и геофизики ДВО РАН, Южно-Сахалинск, Россия, degtyarevvladislav96@yandex.ru

Received 16 January 2025
Accepted 23 February 2025

Поступила 16.01.2025
Принята к публикации 23.02.2025